

Effects of the Addition of Electrolyte on Liquid Infiltration in a Hydrophobic Nanoporous Silica Gel

A. Han,[†] X. Chen,[‡] and Y. Qiao^{*,†}

Department of Structural Engineering, University of California at San Diego, La Jolla, California 92093-0085,
and Department of Civil Engineering and Engineering Mechanics, Columbia University,
New York, New York 10027

Received February 11, 2008. Revised Manuscript Received May 6, 2008

In this letter, we report the experimental results of pressure induced infiltration in the hydrophobic nanopores of a silica gel. The infiltration pressure increases with the prolonged surface treatment time, whereas the infiltration volume is not dependent on the surface coverage. When temperature increases, if the liquid phase is pure water, the infiltration pressure would decrease, which is in agreement with the classic contact angle measurement results at large solid surfaces. As an electrolyte is added, however, the variation in infiltration pressure is negligible over a broad temperature range.

I. Introduction

Nanofluidics behavior has been an active area of research for the past decade.^{1–3} As liquid molecules are confined in a nanometer-sized channel, classic continuum fluid mechanics is no longer relevant, and a number of interesting phenomena have been discovered. According to molecular dynamics (MD) simulations, in a carbon nanotube (CNT) water molecules may form a chainlike structure, and their behavior can be “frictionless”.^{4–7} In some systems, even when the nanochannel surface is nominally wettable to the liquid and a high hydrostatic pressure is applied, there must be a free volume a few times larger than the liquid molecule; otherwise, the liquid cannot enter the channel.^{8,9} The important role of gas molecules was also analyzed.¹⁰ In a nanochannel, a single gas molecule can either “block” the channel or promote liquid molecule diffusion. A cluster of a small number of gas molecules (i.e., a nanobubble) can significantly change the defiltration behavior of a confined liquid. These phenomena can also be explained by a mean-field theory,¹¹ where the liquid infiltration and defiltration are associated with the mass and energy exchanges among solid, liquid, and gas phases.

Whereas previous work in this area has shed much light on the fundamental mechanisms and processes that govern nanofluidic properties, the combined effect of liquid composition and temperature is still relatively uninvestigated. Usually, to observe liquid behavior in nanochannels or nanotubes directly, in situ techniques must be developed using atomic force microscopy

(AFM) or transmission electron microscopy (TEM),^{12–15} which imposes tremendous constraints on sample preparation and handling. Moreover, computer simulation of ion motion and its thermal dependence involves an extensive use of quantum mechanics,^{16–19} which can be prohibitively time-consuming. Recently, a pressure-induced-infiltration (PII) technique was developed so as to investigate nanofluidic behavior on large length and time scales.^{20–24} As a nanoporous material is immersed in a nonwetting liquid, an external pressure must be applied to overcome the capillary effect to force the liquid molecules into the energetically unfavorable nanopores. On the basis of the measurement of infiltration pressure and infiltration volume, the effective solid–liquid interfacial tension can be estimated. By using this technique, the motion of pressurized liquid can be conveniently examined over a broad temperature range.

II. Experimental Section

In the current study, we investigated a surface-treated nanoporous silica gel with a relatively uniform pore size distribution. The network material was obtained from Davisil, and the average particle size was about 250–500 μm . As shown by the dashed line in Figure 1, through a Barret–Joyner–Halenda (BJH) analysis, the average nanopore size was determined to be 16.2 nm. The specific nanopore volume was 1.1 cm^3/g , and the specific surface area was 305 m^2/g . Because it was intrinsically hydrophilic, chlorotrimethylsilane (CTMS) surface treatment was used to modify its surface structure. The details of the treatment procedure have been discussed elsewhere.²⁵ In the surface-treated silica gel, the pore walls were covered with a monolayer of $\text{OSi}(\text{CH}_3)_3$. Because of the high degree

* Corresponding author. E-mail: yqiao@ucsd.edu.

[†] University of California at San Diego.

[‡] Columbia University.

- (1) Eijkel, J. C. T.; van den Berg, A. *Lab Chip* **2005**, *5*, 1202.
- (2) Todd, B. D. *Mol. Simul.* **2005**, *31*, 411.
- (3) Mijatovic, D.; Eijkel, J. C. T.; van den Berg, A. *Lab Chip* **2005**, *5*, 492.
- (4) Sansom, M. S. P.; Biggin, P. C. *Nature* **2001**, *414*, 156.
- (5) Mann, D. J.; Halls, M. D. *Phys. Rev. Lett.* **2003**, *90*, 195503.
- (6) Kalra, A.; Garde, S.; Hummer, G. *Proc. Natl. Acad. Sci. U.S.A.* **2003**, *100*, 10175.
- (7) Majumder, M.; Chopra, N.; Andrews, R.; Hinds, B. J. *Nature* **2005**, *438*, 44.
- (8) Wasan, D. T.; Nikolov, A. D. *Nature* **2002**, *423*, 156.
- (9) Han, A.; Qiao, Y. *J. Am. Chem. Soc.* **2006**, *128*, 10348.
- (10) Qiao, Y.; Cao, G.; Chen, X. *J. Am. Chem. Soc.* **2007**, *129*, 2355.
- (11) Han, A.; Kong, X.; Qiao, Y. *J. Appl. Phys.* **2006**, *100*, 014308.
- (12) Holt, J. K.; Park, H. G.; Wang, Y. M.; Stadermann, M.; Artyukhin, A. B.; Grigoropoulos, C. P.; Noy, A.; Bakajin, O. *Science* **2006**, *312*, 1034.

- (13) Kolesnikov, A. I.; Zanotti, J. M.; Loong, C. K.; Thiyagarajan, P.; Moravsky, A. P.; Loutfy, R. O.; Burnham, C. J. *Phys. Rev. Lett.* **2004**, *93*, 035503.
- (14) Joseph, P.; Cottin-Bizonne, C.; Benoit, J. M.; Ybert, C.; Journet, C.; Tabeling, P.; Bocquet, L. *Phys. Rev. Lett.* **2006**, *97*, 156104.
- (15) Dellago, C.; Hummer, G. *Phys. Rev. Lett.* **2006**, *97*, 245901.
- (16) Xiong, Y.; Zhan, C. G. *J. Phys. Chem.* **2006**, *110*, 12644.
- (17) Wu, W.; Shaik, S.; Saunders, W. H. *Can. J. Chem.* **2005**, *83*, 1649.
- (18) Bernasconi, C. F.; Ali, M.; Nguyen, K.; Ruddat, V.; Rappoport, Z. *J. Org. Chem.* **2004**, *69*, 9248.
- (19) Liao, J. L.; Voth, G. A. *J. Chem. Phys.* **2002**, *116*, 9174.
- (20) Qiao, Y.; Punyamurtula, V. K.; Han, A.; Kong, X.; Surani, F. B. *Appl. Phys. Lett.* **2006**, *89*, 251905.
- (21) Chen, X.; Surani, F. B.; Kong, X.; Punyamurtula, V. K.; Qiao, Y. *Appl. Phys. Lett.* **2006**, *89*, 241918.
- (22) Surani, F. B.; Han, A.; Qiao, Y. *Appl. Phys. Lett.* **2006**, *89*, 093108.
- (23) Surani, F. B.; Qiao, Y. *J. Appl. Phys.* **2006**, *100*, 034311.
- (24) Surani, F. B.; Kong, X.; Qiao, Y. *Appl. Phys. Lett.* **2005**, *87*, 251906.
- (25) Han, A.; Qiao, Y. *Chem. Lett.* **2007**, *36*, 882.

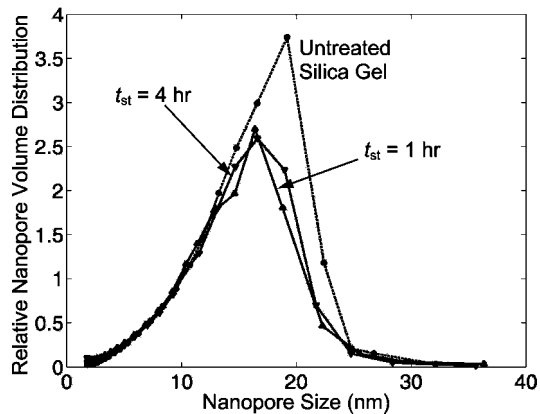


Figure 1. BJH analysis of the nanopore volume distribution.

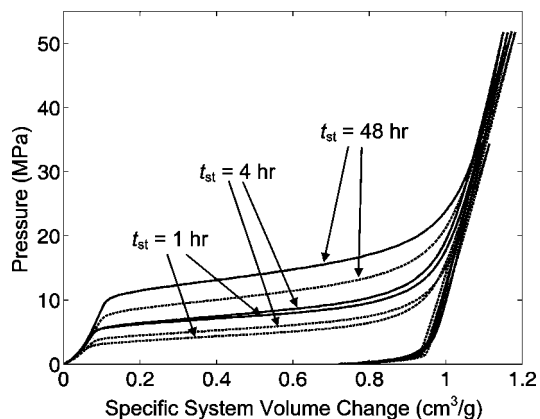


Figure 2. Typical sorption isotherm curves at room temperature. The solid and dashed curves indicate the behavior of systems based on sodium chloride solution and pure water after various surface treatment times, respectively.

of hydrophobicity of methane groups, the nanopore surface became nonwetttable to water. The specific nanopore volumes are 9.9, 9.2, 9.6, and 9.4 cm³/g, and the specific surface areas are 240, 232, 229, and 216 m²/g after modification for 1, 4, 30, and 48 h, respectively. The effective pore size is around 15.5 nm after the surface modification, as shown by the solid lines in Figure 1.

The PII testing sample was prepared by immersing 0.5 g of surface-treated silica gel in 7 g of liquid in a stainless steel cylinder. The liquid phase was either deionized water or a saturated aqueous solution of sodium chloride (26.4% at 273 K under 1.01×10^5 Pa). The steel cylinder was sealed by a steel piston equipped with a gasket. Using a type 5582 Instron machine, the piston was compressed into the cylinder, applying quasi-hydrostatic pressure on the liquid phase. To avoid possible internal friction effects,²⁶ the loading rate was set to 0.5 mm/min., which could be regarded as quasi-static because lowering it further did not cause detectable variations in experimental data. When the pressure exceeded about 50 MPa, the piston was moved back at the same rate until the pressure decreased to zero. During the loading–unloading process, the pressure was calculated from $P = F_p/A_p$, with F_p being the piston force measured by a 50 kN load cell and $A_p = 286$ mm² is the cross-sectional area of the piston; the specific system volume change was calculated from $\Delta V = d_p(A_p/m)$, with d_p being the piston displacement and $m = 0.5$ g being the mass of silica gel. The experiments were carried out either at ambient temperature or at elevated temperatures. The temperature was controlled by a water bath. Typical sorption isotherm curves are shown in Figures 2 and 3. Because the confined liquid did not defiltrate, after the first loading cycle the nanopores would remain

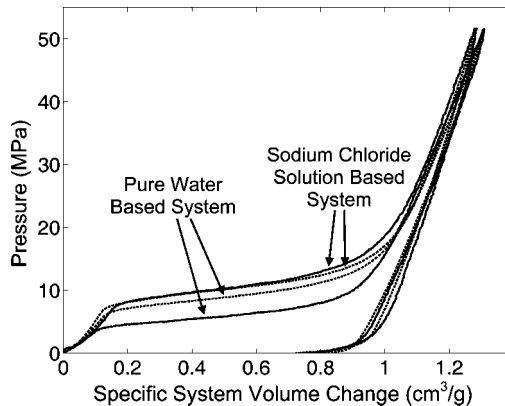


Figure 3. Typical sorption isotherm curves at various temperatures. The dashed and solid curves indicate the results at room temperature (20 °C) and at an elevated temperature (80 °C), respectively.

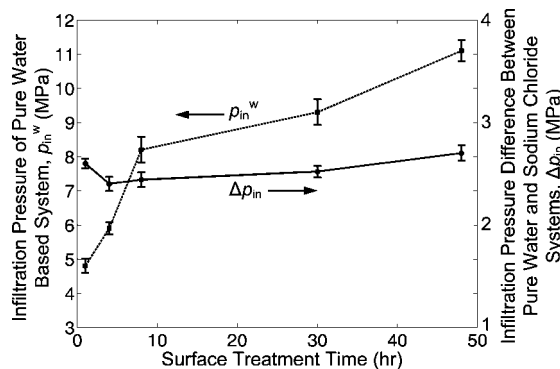


Figure 4. Infiltration pressure increase caused by the addition of sodium chloride. The dashed line indicates the infiltration pressures of pure-water-based systems. The solid line indicates the difference between the infiltration pressure based on the pure-water system and that based on the electrolyte system.

occupied, and no infiltration could take place from the second cycle. Therefore, the following discussion will be focused on the system performance at the first loading.

III. Results and Discussion

At the beginning of a PII experiment, when the pressure is relatively low the liquid phase cannot infiltrate into the nanoporous silica gel, and the slope of the sorption isotherm curve reflects the compressibility of the liquid and empty silica particles. When the pressure is sufficient to overcome the capillary effect, the liquid starts to enter the nanopores, causing the formation of a wide infiltration plateau. If the nanopore size distribution were perfectly uniform, the infiltration plateau should be flat. In the current study, because of the pore size distribution, the slope is finite. Eventually, when the nanopores are filled, the system compressibility becomes small again. The slope of the high-pressure linear compression stage is larger than that in the low-pressure stage, indicating that the empty silica particles are more compliant than the filled ones.

According to Figure 2, the infiltration pressure, p_{in} , which for self-comparison purposes can be defined as the pressure at the middle point of the infiltration plateau, increases with surface treatment time, t_{st} (see also the dashed line in Figure 4). During surface treatment, CTMS molecules diffuse into the nanopores and react with the hydroxyl sites. As t_{st} increases, more silane groups can attach to the nanopore walls, which causes an increase in the degree of hydrophobicity. The average effective nanopore size decreases to 15.5 nm after the CTMS modification and it

(26) Surani, F. B.; Kong, X.; Panchal, D. B.; Qiao, Y. *Appl. Phys. Lett.* **2005**, *86*, 151919.

does not change much with increasing t_{st} . Using the classic Laplace–Young equation, the excess solid–liquid interfacial tension can be assessed as $\Delta\gamma = p_{in}(r/2)$, where $r \approx 7.8$ nm is the effective pore radius. In the pure-water-based system where t_{st} is 1 h and p_{in} is about 4.6 MPa, $\Delta\gamma$ is about 18 mJ/m²; when t_{st} is 4 h and p_{in} is about 5.9 MPa, $\Delta\gamma$ is nearly 23 mJ/m²; and when t_{st} is 48 h and p_{in} is about 11.3 MPa, $\Delta\gamma$ is about 44 mJ/m². These data are quite plausible compared with the data of large solid surfaces.²⁷ If $t_{st} > 48$ h, further increase in treatment time would not result in a detectable variation in p_{in} , suggesting that the surface coverage saturates.

The infiltration volume, $\Delta V_p = 0.82$ cm³/g (i.e., the width of the infiltration plateau) is quite insensitive to the treatment time, as shown in Figure 2. That is, the volume of porous space that can be accessed by liquid molecules is not related to the surface coverage. This suggests that the confined liquid molecules can access the “free” space between the surface groups, regardless of the density of the silane groups, the details of which are still quite unclear. Because defiltration does not occur even when $t_{st} = 48$ h and the surface group layer saturates, the irreversibility of the infiltration process should not be associated with the uniformity of the surface layer.²⁸

When sodium chloride is added to the liquid phase, the infiltration pressure increases, as shown by the solid lines in Figures 2 and 4. Compared with the data of the pure-water-based system, no variation in infiltration volume can be detected, as it should be because the specific nanopore volume does not vary. As the surface treatment time changes from 1 to 48 h, compared with the pure-water-based system the increase in infiltration pressure, Δp_{in} , changes quite randomly in a relatively small range around 2.5 MPa, indicating that it is not dependent on the surface coverage and the absolute value of solid–liquid interfacial tension. Using the Laplace–Young equation, the corresponding variation in effective solid–liquid interfacial tension, $\delta\gamma$, can be estimated to be about 10 mJ/m², which is equal to the previous data obtained from the isotherm curves of surface-treated MCM-41, whose average nanopore size is 2.8 nm.²⁹ The value of 10 mJ/m² is quite large compared with the increase in surface tension of the liquid phase,²⁷ which may be related to the unique ion distribution in the nanoenvironment. As shown in Figure 5a, once a large solid surface is exposed to an electrolyte solution the ions near the solid surface are subjected to unbalanced forces from solid and liquid molecules/atoms.³⁰ As a result, the liquid structure is no longer homogeneous. Immediately adjacent to the solid surface, the solvated ions are quite ordered, and the ion density is high. Because of the attraction forces from the counter charges in the solid, these ions are relatively immobile. This layer is often referred to as the Stern layer. Outside the Stern layer, the ion structure is less ordered, and the density is lower (but still higher than that in the bulk phase), which is often referred to as the Gouy–Chapman layer. The interface zone thickness is typically in the range of several angstrom to several nanometers, depending on solid and liquid materials, ion concentration, and species as well as configurations of clusters of water molecules. Beyond the interface zone, the ion distribution is random. In a nanopore, as shown in Figure 5b, the ion distribution is constrained by the pore wall. With the same nominal ion concentration, the effective surface ion density is higher than that at a large solid surface, resulting in a more pronounced interfacial tension increase.

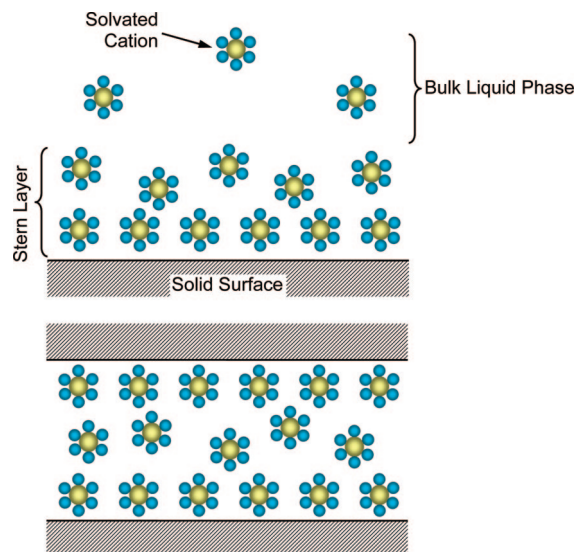


Figure 5. Schematic diagrams of ion distributions (a) at a large solid surface and (b) in a nanopore. Free water molecules and unsolvated ions are not shown.

With pure water, the solid–liquid tension is dominated by the structure of water molecules near the solid surface. The interface zone thickness is relatively small. Thus, in the nanoporous silica gel under investigation, the solid–liquid interface structure is similar to that at a large solid surface, which explains why the testing results of the p_{in} – t_{st} relationship of water-based systems agree with the literature data. Moreover, as temperature rises, as shown in Figure 3, the infiltration pressure decreases significantly. When the temperature is 80 °C, the water molecules are more mobile in the nanopore and overcome the infiltration energy barrier much more easily. Compared with the testing result at ambient temperature, p_{in} is reduced by nearly 30% from around 9.2 to 6.4 MPa, which again fits the contact-angle measurement results for large solid surfaces.²⁷

In the saturated sodium chloride-solution-based system, however, temperature change has little influence on the infiltration pressure (Figure 3). Because previous testing data demonstrated that in nanopores the effective interfacial tension was strongly dependent on the electrolyte concentration,³¹ the observed insensitive of infiltration pressure should be attributed to the reduced thermal dependence of effective ion density at nanopore surfaces. At a large solid surface, as temperature increases, it is relatively easy for the solvated ions to diffuse away from the interface zone, and thus the interface ion density would decrease, causing a considerable decrease in interfacial tension, which is well known as the thermocapillary effect.³² In a nanopore, because of the unique structure of solvated ions, the effective interface ion density may not be as sensitive to temperature as at a large solid surface. The Debye length of saturated NaCl is around 0.4 nm, and in a nanopore the double length (from both sides) is around 1 nm. Even though an interior phase may exist in the middle part of the nanopore, its volume is only 4 to 5 times larger than the volume occupied by the surface layer, which is much smaller than the bulk phase at a large solid surface. Therefore, it may not be able to serve as an infinitely large ion “reservoir”; that is, the diffusion along the radius direction at solid–liquid surfaces in nanopores is suppressed. Even if equilibrium can eventually be reached between the interior of nanopores and the

(27) Hartland, S., Ed.; *Surface and Interfacial Tension*; Surfactant Science Series; Marcel Dekker: New York, 2004.

(28) Lim, M. H.; Stein, A. *Chem. Mater.* **1999**, *11*, 3285.

(29) Han, A.; Qiao, Y. *Langmuir* **2007**, *23*, 11396.

(30) Ibach, H. *Physics of Surfaces and Interfaces*; Springer: New York, 2007.

(31) Kong, X.; Surani, F. B.; Qiao, Y. *Phys. Scr.* **2006**, *74*, 531.

(32) Myers, D. *Surfaces, Interfaces, and Colloids: Principles and Applications*, 2nd ed.; Wiley-VCH: New York, 1999.

surrounding liquid phase, the characteristic time of ion diffusion along the axial direction can be much longer than that of the pressure-induced infiltration experiment.³³ Because along the axial direction the ion structure is quasi-periodic, the effective ion density would not vary much until the kinetic effect becomes pronounced.

IV. Conclusions

In summary, the current study is focused on the PII experiment on a surface-treated nanoporous silica gel. The

infiltration pressure increases with increasing surface treatment time for both pure water and electrolyte-solution-based systems. The infiltration volume is not dependent on the surface coverage. The effective interfacial tension is thermally dependent on the pure-water-based system but insensitive to temperature change in the electrolyte-solution-based system. These phenomena can be attributed to the confinement effect of pore walls in the nanoenvironment.

Acknowledgment. This work was supported by the Army Research Office under grant no. W911NF-05-1-0288.

LA800446Z

(33) Qiao, Y.; Kong, X. *Phys. Scr.* **2005**, *71*, 27.